SEBHA UNIVERSITY JOURNAL OF PURE & APPLIED SCIENCES VOL.21 NO. 2 2022
DOI: 10.51984/JOPAS.V21I2.2059

مجلة جامعة سبها للعلوم البحتة والتطبيقية
Sebha University Journal of Pure & Applied Sciences

Journal homepage: www.sebhau.edu.ly/journal/index.php/jopas

Soret Dissipation Effect On Heat And Mass Transmission Of Non-Newtonian Casson Radiative Nanofluid Flow With Lorentz Drag And Rosseland Radiation

*Uka Uchenna Awucha[a], Amadi Okechukwu[b]

[a] Department of Basic Sciences, School of Science and Technology, Babcock University, P.M.B 4003. Ilishan-Remo, Ogun State, Nigeria.
[b] Department of Mathematics, Ignatius Ajuru University of Education, Rumuolumeni, Portharcour, Rivers State, Nigeria.

Keywords:
Heat Transmission
Mathematica Software
Magnetohydrodynamic
Radiation
Soret Impact
Series Approximation Technique

ABSTRACT

The goal of the current study considers the impact of Lorentz force and radiation on the reactive Casson-Nanofluid flow over a flow over a stretched surface with Soret impact. However, its industrial and technological applications are numerous but not limited to solar power, glass spinning, nuclear reactors, processing and packaging of food, etc. The flow being considered is a function of the stretched surface along its direction in line with a linearly changing velocity with such distance from a given immovable point. The partial differential equations describing the momentum, energy (heat) and mass transfer equations were transformed into non-linear ordinary differential equations in non-dimensional forms through the use of the similarity variables approach. The solution which was carried out through the application of the series approximation method is presented analytically. However, the Mathematica software was used in obtaining the numerical solutions. Thus, the impacts of physical parameters of the fluid were studied. The results indicated that: the velocity of fluid flow lessens due to the combined intensification of values of the non-Newtonian Casson fluid and magnetic field parameters. An upsurge in Grashof heat and radiation factors yields a rise in the velocity. Influence of collective Casson and magnetic parameters leads to an appreciation of heat distribution. Also, the concentration field declines as both the Casson and Schmidt parameters improve. The diminishing distribution fields of both the wall energy and mass gradients are functions of the appreciating values of the non-Newtonian number.

تأثير تبديد سورت على انتقال الحرارة والكتلة لتدفق كاسون نانوفولويد غير النيوتوني مع التأثير المشترك لسحب لورنتز واشعاع روسلاند

*أوكا أوشينا أوشا[1] و حمدي أوكيشوكو[2]

[1] قسم العلوم الأساسية ، كلية العلوم والتكنولوجيا ، جامعة بابكوك ، *P.M.B 4003*. إليشان - ريمو ، ولاية أوجون ، نيجيريا.
[2] قسم الرياضيات ، جامعة إغناتيوس أجورو للتعليم ، رومولوميني ، بورثاركور ، ولاية ريفرز ، نيجيريا.

الكلمات المفتاحية:
انتقال الحرارة
برنامج Mathematica
مغناطيسي هيدروديناميكي (MHD)
تأثير Soret
التقريب المتسلسل
تقنية
إشعاع

الملخص

يأخذ هذا التحليل في الاعتبار تأثير قوة لورنتز والإشعاع على تدفق كاسون-نانوفلويد التفاعلي عبر تدفق فوق سطح ممتد مع تأثير سورت. تتعدد التطبيقات الصناعية والتكنولوجية لهذه الدراسة ولكنها لا تقتصر على الطاقة الشمسية ، والغزل الزجاجي ، والمفاعلات النووية ، وتجهيز وتعبئة المواد الغذائية ، وما إلى ذلك. يعتبر التدفق الذي يتم اعتباره دالة للسطح الممتد على طول اتجاهه بما يتماشى مع خطي. السرعة المتغيرة بهذه المسافة من نقطة ثابتة معينة. تم تحويل المعادلات التفاضلية الجزئية التي تصف معادلات الزخم والطاقة (الحرارة) ونقل الكتلة إلى معادلات تفاضلية عادية غير خطية في أشكال غير أبعاد من خلال استخدام نهج متغيرات التشابه. تم عرض الحل الذي تم تنفيذه من خلال تطبيق طريقة التقريب المتسلسل بشكل تحليلي. ومع ذلك ، تم استخدام برنامج Mathematica في الحصول على الحلول العددية. وهكذا ، تم دراسة تأثير العوامل الفيزيائية للسائل. أشارت النتيجة إلى أن سرعة تدفق المائع تقل بسبب التكثيف المشترك لقيم مائع كاسون غير النيوتوني ومعلمات المجال المغناطيسي. تؤدي زيادة عوامل الحرارة والإشعاع في Grashof إلى زيادة السرعة. يؤدي تأثير الكاسون

*Corresponding author:
E-mail addresses: ukau@babcock.edu.ng ,(A. Okechukwu) agirobert@yahoo.com
Article History : Received 04 September 2022 - Received in revised form 09 December 2022 - Accepted 12 December 2022

الجماعي والمعلمات المغناطيسية إلى تقدير توزيع الحرارة. أيضًا ، ينخفض مجال التركيز مع تحسن كل من معلمات Casson و Schmidt. يؤدي تأثير الزيادة في رقم كاسون إلى ارتفاع معامل احتكاك الجلد.

Introduction

Nanofluid flow past a stretched sheet finds its applicability in several engineering processes This is evident in the production of a stretching sheet interrelating mechanically and thermally with a fluid whose temperature is ambient. Under this phenomenon, the flow performance far from the strectched material is vital as long as the cooling rate of the sheet is concerned. The rate at which temperature flows forms is of great concern and importance to several industries for efficient and greater mechanical efficiency, for example in the process of cooling of nuclear radiators, power sourcing equipment such and its mechanisms.Heat transmission occurs in different forms as convection, conduction and radiation. Each of these means of conveyance of thermal energy in a given system differes from one another. However, for heat and diffusion transporting processes to necessary and could exist in form be effective, a medium becomes of a fluid. Thus, a substance or material which either flows or exhibits an unceasing distortion arising from the shear strain is termed a fluid. This implies that a fluid displays a zero-shear modulus. Therefore, air, water, ethylene glycol (ECG), engine oil etc., are examples of fluid. Casson fluid represents a shear diminishing fluid which exhibits an endless viscosity at zero proportion of such shear, without viscosity at a limitless shear proportion, [1]. Meanwhile, the jelly, tomato sauce, honey, saturated fruit juice etc., have such characteristics. It is needful to state that solids are not fluids although some acts as such. For example, pitch has greater viscosity that enables it to flow slowly, and silly putty also flows though becomes solidified when it comes in contact with a sharp force. According to some studies, water has served as a means through which heat can be transferred. Similarly, breakthroughs in research have revealed that the thermal conductivity of water can be improved by introducing finely divided particles of metals, metallic oxides in the measure of $1-100$ nanometre etc., in it. Thus, this led to a concept called Nanofluid. The innovation of nanofluid is attributed to [2] for his quest in studying new evidences for achieving lessening proportion of heat deposited in electrical and mechanical devices. The significance of this study ranges from its application to the metallurgical, plastic (PVCs), manufacturing firms, polymer production process, galvanisation of cables and in spinning of glasses etc. [3], investigated the influence of chemical reactivity and radiation on MHD Nanofluid flow over an exponentially elastic plate by applying the perturbation method. They opined that improvement of the elastic plate is a function of increasing speed of flow. The analysis of both the natural and forced convective angular velocity fluid transfer over an exponentially expanding plate was done by [4]. Subsequently, [5] examined the impact of fractional slip flow over an exponentially elongated material while [6] analysed a three-dimensional flow of a second rating fluid near a non-static plate. The problem of hydromagnetic nanofluid drift past an exponentially elastic plate under the effect of radiation and inhomogeneous thermal source/sink was solved by [7]. Also, [8] explained the motion of a fluid-based nanofluid past a curly material in a porous medium. However, it is necessitating to mention that the advantage of suction and blowing studies and procedures in so many spheres of engineering include but not limited to the designing of thrust comportment for airplanes and also as well as in centrifugal diffusers. Thus, [9] examined the heat transmission structures via a stormy magnetohydrodynamic Casson fluid. In the same way, the study of Casson liquid flow with entropy source and sway of hall flux was carried out by [10]. An approximation approach involving the application of homotopy analysis method (HAM) was used in examining nanofluid exemplary results as a result of its movement [11]. In their quest towards contribution of knowledge, [12, 13] proposed a model for mathematical replication in bioengineering project in contractility with nanofluids in a Newtonian case. Thereafter, [14] extended the work by considering the non-Newtonian condition just as [15], also put an extension of the study by laying emphasis on the issue of lessening material. The examination of thermal spreading structures of Casson flow in the presence of radiative heat and permeable medium is attributed to [16]. Similarly, [17] studied the three dimensional (3D) of energy and effusion transmission of fluid flow past a delicate material immersed in an absorbent instrument. Their work captured both flow and heating descriptions at various temperature gradients points. They opined that increment in the Casson number leads to the enlargement of the momentum and heat boundary walls.

A thorough numerical analysis of MHD radiation mixture of metallic (ferro) fluid drift with thermal gradient for the description of thermal transfer processes has been described [18]. However, [19] investigated the radiation effect on time-changing hydromagnetic liquid flow through a holey sheet. Their results pointed out that the solidification of thermal boundary layer is as a result of enhancing the radiation parameter. Also, [20] examined the unsteady magnetohydrodynamic heat and mass transmission of chemically reactive dual-diffusive Casson fluid flow over a flat plate engrossed in a spongy medium. The movement of heat and mass transport in magnetohydrodynamic Casson fluid past an exponentially expanding porous surface has been conducted through the use of Matlab bvp4c software [21]. According to their result, increasing the exponential and thermal generation factors improves the rate of thermal transportation. The analytical simulation of heat and mass transference in Casson fluid distribution over an elastic material through the deployment of the HAM was studied, [22]. Their result is indicative of the fact that velocity decreases as the Casson parameter increases while the electric charge in the conducting fluid contributed in enhancing the temperature. Due to the importance of fluid flow studies, [23] analysed the MHD 3D Casson fluid flow over a permeable linearly elastic material.

The afore mentioned analysis is limited to the study of heat and mass transferring behaviour of non-Newtonian fluid with elastic sheet. Hence, in this present work, a numerical investigation on energy and mass transmission fluid flow over a stretched plate with combined effect of non-Newtonian and Lorentz factors, Rosseland radiation as well as thermal Grashof parameters impacts are considered. The nonlinear boundary layer equations in partial differential equation forms are resolved into coupled ordinary differential equations. The series approximation and integrating factor approaches are applied in the solution process. The results and effect of various physical fluid quantities are presented in graphical form and were obtained with the aid of the Mathematica software application. Hence, the legends are presented and our results discussed.

Mathematical Formulation of Equations

A steady incompressible viscous nanofluid flow involving a stretched plate at $y = 0$ (plane) with suction. Fluid transfer is kept at $y > 0$. The application of the same and opposite forces towards the $x - axis$ is made in such a way that the origin remains immovable as the wall is over-extended. This is depicted in figure 1. However, for an isotropous drift of a well-known Casson fluid, we have its viscoelastic model given below as:

$$\tau_{ij} = \begin{cases} 2\left(\mu_B + \frac{P_y}{\sqrt{2\pi}}\right)e_{ij}, & \pi > \pi_c \\ 2\left(\mu_B + \frac{P_y}{\sqrt{2\pi}}\right)e_{ij}, & \pi < \pi_c \end{cases} \quad (1)$$

Such that the constituent $e_{ij} = (i,j)th$ represents the proportion of distortion, $\pi =$ product of the constituent of distortion ratio through itself i.e., $\pi = e_{ij}e_{ij}$ and $\pi_c =$ critical value of the product hinged on the non-Newtonian equation, μ_B and P_y refers to the malleable active viscidity and yield strain of the non-Newtonian fluid respectively. However, an extension of the work of [24] has been done with the attention on the nanoparticle specie concentration, heat Grashof number effect and thermo-diffusion on the boundary. Thus, the equations are modelled as follows:

$$\frac{\partial u}{\partial x} + \frac{\partial u}{\partial y} = 0 \quad (2)$$

$$\frac{\partial p}{\partial x} + u\frac{\partial u}{\partial x} + v\frac{\partial u}{\partial y} = p\left(1 + \frac{1}{\lambda}\right)\frac{\partial^2 u}{\partial y^2} - \frac{\sigma B_0^2}{\rho}u + g\beta_c(T - T_\infty) \quad (3)$$

$$u\frac{\partial T}{\partial x} + v\frac{\partial T}{\partial y} = \frac{k}{\rho c_p}\frac{\partial^2 T}{\partial y^2} + \frac{\lambda\sigma B_0^2}{\rho}(T - T_\infty) - \frac{k}{\rho c_p}\frac{\partial qr}{\partial y} \quad (4)$$

$$u\frac{\partial C}{\partial x} + v\frac{\partial C}{\partial y} = D_B\frac{\partial^2 C}{\partial y^2} + \frac{D_f K_T}{T_m}(T - T_\infty) \quad (5)$$

In relation on:

$$y = 0: u = U_s, v = -w_o, T = T_s, C = C_s \quad (6)$$

$$y \to \infty: u = v \to 0, T \to T_\infty, C \to C_\infty \quad (7)$$

However, the diagram representation follows thus;

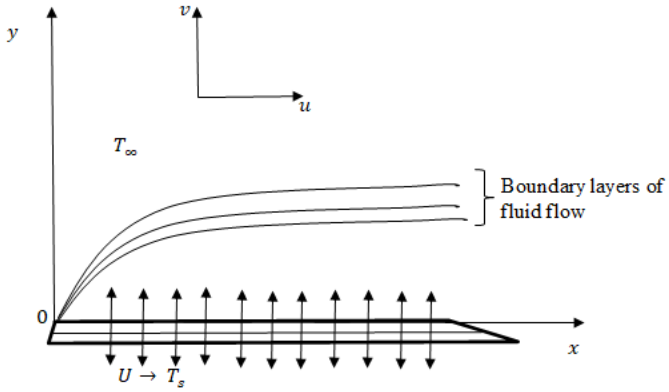

Figure 1. Diagrammatical representation of the flow geometry.

From equations (2) to (5), the velocity components along the x and y axes are u and v, $\nu =$ kinematic viscosity, $\lambda = \mu_B\sqrt{\frac{2\pi_c}{p_y}}$ is the Casson (non-Newtonian) fluid number, $T, T_m, k, q, c_p, \beta_c, k_f, \rho, D_f, \sigma, D_B$ and k_T are average thermal capacitance, heat extension coefficient, nanofluid heat capacitance, fluid density, mass diffusivity of nanofluid, electrical conductivity, coefficient of mass diffusivity as well as diffusivity proportion.

Method of Solution

We shall solve the problem under consideration to obtain its analytical solution through the application of the series approximation method. Then, the numerical simulation was achieved by using the Mathematica V10 package as it's been adjudged to be reliable, effective and use-friendly. Therefore, applying the Rosseland approximation for qr, we obtain

$$qr = -\left(\frac{4\sigma^*}{3k^*}\right)\frac{\partial T^4}{\partial y} \quad (8)$$

Such that σ^* and k^* signifies Stafan-Boltzmann parameter and average absorption coefficient. If the temperature gradient around the flow occurs in such a way that T^4 can be expanded by applying the Taylor series with expansion of T^4 at T_∞ with the exclusion of the higher order terms, then we have $T^4 \equiv 4T_\infty^3 T - 3T_\infty^4$ such that equation (4) becomes,

$$u\frac{\partial T}{\partial x} + v\frac{\partial T}{\partial y} = \frac{k}{\rho c_p}\frac{\partial^2 T}{\partial y^2} + \frac{\lambda\sigma B_0^2}{\rho}(T - T_\infty) - \frac{16T_\infty^4}{3\rho c_p k^*}\frac{\partial^2 T}{\partial y^2} \quad (9)$$

Were,

$w_o(x) > 0$ implies suction and $w_0(x) < 0$ refers to blowing velocities. The following similarity variables are deployed in transforming the equations (2), (3), (5) and (9) respectively.

$$\varphi = \sqrt{\nu U_\infty x}\ Z(\eta), u = U_\infty\frac{dz}{d\eta}, v = \frac{1}{2}\sqrt{\frac{\nu U_\infty}{x}}\left(\eta\frac{dz}{d\eta} - z(\eta)\right),$$

$$\eta = \frac{y}{\sqrt{\frac{\nu x}{U_\infty}}}, \theta(T_s - t_\infty) = T - T_\infty, \emptyset(C_s - C_\infty) = C - C_\infty, \quad (10)$$

$$u\frac{\partial\varphi}{\partial y}, v = -\frac{\partial\varphi}{\partial x}$$

Putting equation (10) into equations (2), (3), (5) and (9), we have

$$(1 + \lambda^{-1})\frac{d^3Z}{d\eta^3} + \frac{1}{2}Z(\eta)\frac{d^2Z}{d\eta^2} - H\frac{dZ}{d\eta} + G_t\theta(\eta) = 0 \quad (10)$$

$$\left(1 + \frac{4}{3}Nr\right)\frac{d^2\theta}{d\eta^2} + PrZ(\eta)\frac{d\theta}{d\eta} + \lambda H\theta(\eta) = 0 \quad (11)$$

$$\frac{d^2\emptyset}{d\eta^2} + \frac{1}{2}ScZ(\eta)\frac{d\emptyset}{d\eta} + ScSr\theta(\eta) = 0 \quad (12)$$

$$\eta = 0; Z = w_o, Z' = 1, \theta = 1, \emptyset = 1 \quad (13)$$

$$\eta \to \infty; Z' \to 0, h \to 0, S \to 0$$

According to [25], the following descriptions are applied to solving the problem.

$$\eta = \zeta w_o, z(\eta) = w_o Z(\eta), \theta(\eta) = h(\eta), \emptyset(\eta) = S(\eta), \delta = \frac{1}{w_o^2}$$

Using the relation above and its derivatives in equations (10) to (12) yields

$$(1 + \lambda^{-1})\frac{d^3Z}{d\eta^3} + \frac{1}{2}Z(\eta)\frac{d^2Z}{d\eta^2} - H\frac{dZ}{d\eta} + G_t\theta(\eta) = 0 \quad (14)$$

$$\left(1 + \frac{4}{3}Nr\right)\frac{d^2\theta}{d\eta^2} + PrZ(\eta)\frac{d\theta}{d\eta} + \lambda H\theta(\eta) = 0 \quad (15)$$

$$\frac{d^2\emptyset}{d\eta^2} + \frac{1}{2}ScZ(\eta)\frac{d\emptyset}{d\eta} + ScSr\theta(\eta) = 0 \quad (16)$$

Subject to:

$$\eta = 0; Z = 1, Z' = \delta, h = 1, S = 1$$

$$\eta \to \infty; Z' \to 0, h \to 0, S \to 0 \quad (17)$$

Due to the case of suction, $\delta \ll 1$, the solution of equations (14) to (16) takes the following forms:

$$\left.\begin{aligned} Z(\eta) &= 1 + \textstyle\sum_{i=j=1}^{\infty}\delta^i Z_j(\eta) \\ h(\eta) &= \textstyle\sum_{i=j=1}^{\infty}\delta^i h_j(\eta) \\ S(\eta) &= \textstyle\sum_{i=j=1}^{\infty}\delta^i S_j(\eta) \end{aligned}\right\} \quad (18)$$

Substituting equations (18) and its differentials into equations (14) to (16) and equating the coefficients of corresponding index produces;

$$\left(1 + \frac{4}{3}Nr\right)\frac{d^2h_0}{d\eta^2} + Pr\frac{dh_0}{d\eta} = 0; h_0(0) = 1, h_0(\infty) = 1 \quad (19)$$

$$\frac{d^2S_0}{d\eta^2} + \frac{1}{2}Sc\frac{dS_0}{d\eta} = 0; S_0(0) = 1, S_0(\infty) = 0 \quad (20)$$

$$\left.\begin{aligned} &(1 + \lambda^{-1})\frac{d^3Z_1}{d\eta^3} + \frac{1}{2}\frac{d^2Z_1}{d\eta^2} = 0;\ \ Z_1(0) = 0 \\ &Z_1'(0) = 1, Z_1'(\infty) = 0 \end{aligned}\right\} \quad (21)$$

$$\left(1 + \frac{4}{3}Nr\right)\frac{d^2h_1}{d\eta^2} + Pr\frac{dh_1}{d\eta} + PrZ_1(\eta)\frac{dh_0}{d\eta} + \lambda Hh_0(\eta) = 0$$

$$h_1(0) = 0, h_1(\infty) = 0 \quad (22)$$

$$\frac{d^2S_1}{d\eta^2} + \frac{1}{2}Sc\frac{dS_1}{d\eta} + \frac{1}{2}ScZ_1(\eta)\frac{dS_0}{d\eta} + ScSrh_0(\eta) = 0$$

$$S_1(0) = 0, S_1(\infty) = 0 \quad (23)$$

$$\left.\begin{aligned} &(1 + \lambda^{-1})\frac{d^3Z_2}{d\eta^3} + \frac{1}{2}\frac{d^2Z_2}{d\eta^2} + \frac{1}{2}Z_1(\eta)\frac{d^2Z_1}{d\eta^2} - H\frac{dZ}{d\eta} = 0 \\ &Z_2(0) = 0, Z_2'(0) = 0, Z_2'(\infty) = 0 \end{aligned}\right\} \quad (24)$$

It is important to note that, Nr, Pr, Sc, λ, H and Sr indicates radiation, Prandtl, Schmidt, non-Newtonian, Hartmann and Soret numbers respectively. Solving equations (19) to (24) with the corresponding boundary conditions, we realized the following analytical solutions for the velocity, temperature and nanoparticle concentration of the Casson-nanofluid flow.

$$z'(\eta) = e^{-B\eta} + \delta\left(-\frac{\lambda}{2B(\lambda+1)}\eta e^{-B\eta} + \frac{\lambda}{2B^2(\lambda+1)}e^{-B\eta} - \frac{\lambda}{4B^2(\lambda+1)}e^{-2B\eta} - \frac{\lambda H}{B(\lambda+1)}\eta e^{-B\eta} + \frac{\lambda H}{B^2(\lambda+1)}e^{-B\eta} + \frac{C_4}{B} - BC_6e^{-B\eta} - \frac{\lambda Gt}{q(q-B)(\lambda+1)}e^{-q\eta}\right) \quad (26)$$

$$h(\eta) = e^{-q\eta} + \delta\left(-\frac{q}{B}\eta e^{-q\eta} - \frac{q^2}{B^2(B+q)}e^{-(B+q)\eta} + \frac{3\lambda H}{q(3-4N)}\eta e^{-q\eta} + \frac{A_3}{q} + A_4e^{-q\eta}\right) \quad (27)$$

$$s(\eta) = e^{-\frac{1}{2}Sc\eta} + \delta(-\frac{(Sc)^2}{2B}\eta e^{-\frac{1}{2}Sc\eta} - \frac{(Sc)^2}{2B^2(2B+Sc)}e^{-\left(B+\frac{1}{2}Sc\right)\eta} - \frac{2ScSr}{q(2q-Sc)}e^{-q\eta} + \frac{2K_3}{Sc} + K_4e^{-\frac{1}{2}Sc\eta}) \quad (28)$$

Were,

$$A_3 = 0,\quad A_4 = \frac{q^2}{B^2(B+q)},\ B = \frac{\lambda}{B(\lambda+1)},\quad C_4 = 0,$$

$$C_6 = \frac{\lambda}{B^3(\lambda+1)}\left(\frac{1}{4}+H\right) - \frac{\lambda Gt}{Bq(q-B)(\lambda+1)}, K_3 = 0, K_4 = \frac{(Sc)^2}{2B^2(2B+Sc)} + \frac{2ScSr}{q(2q-Sc)}, q = \frac{3Pr}{3+4N}$$

1**. Nusselt Number**

Of interest to the engineering science field is the coefficient of heat transmission at the wall (Nusselt number) which is given as:

$$h'(0) = \left(\frac{\partial h}{\partial \eta}\right)_{\eta=0} \quad (29)$$

2. **Sherwood Number**

This is expressed as the ratio of the rate of mass transfer across the wall and it is given as

$$S'(0) = \left(\frac{\partial s}{\partial \eta}\right)_{\eta=0} \quad (30)$$

Steps Adopted in the Application of the Mathematica Software

- Installation of the Wolfram Mathematica software in the system.
- The installed Wolfram Mathematica software and notebook worksheet are opened on the system.
- We input the "clear" statement/syntax followed by the various fluid parameters enclosed in a square bracket and followed by the syntax ";". This is done in order to delete any previous work which may lead to a wrong output (solution).
- We declared or stated all the values of the constants obtained in the course of solving the problem analytically and end it with the syntax ";".
- We input the analytical solutions which have been obtained followed by the statement "plot", followed by a square bracket, curly bracket and values of the various fluid parameters including η which are separated by comma and underscore, then enclosed all with a square bracket followed by a curly bracket. At this point, we simulated the programmed language to obtain each graph and legend corresponding to the influence of a parameter that has been varied.

We repeated the simulation processes for each of the fluid parameters in order to ascertain their impact on the rate of flow, temperature as well as nanoparticle concentration.

Results and Discussion

3. **Figures and Tables**

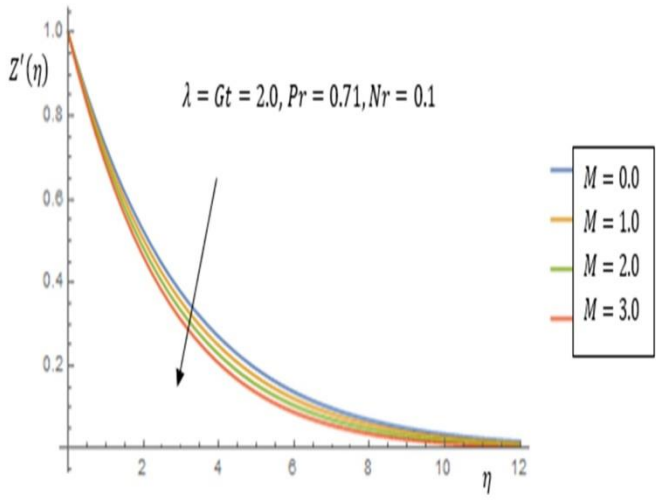

Figure 1. Effect of Magnetic parameter, M on Velocity

Figures 1 to 6, represents the velocity distribution fields with the bearing of various physical fluid parameters. As such, the effect of the magnetic field constraint, M on the rate of flow (velocity) is represented in Figure 1. It can be seen that the fluid velocity decreases as the magnetic number, M is increased. This is attributed to the fact that this parameter possesses a special force (Lorentz force) which tends to regulate and resist the fluid motion by acting in an opposite way thereby leading to a decline in fluid velocity and impediment on the fluid pace. This phenomenon is captured in figure 1. In Figure 2, the radiation parameter, Nr impaction on the velocity is visible. Due to thermal transmission processes in the fluid and its nanoparticles, the rate of heat dispersal improves and the wall becomes thickened thereby leading to a surge in fluidity passage.

The evolution of the combined effects of magnetic, M and radiation, Nr parameters on the fluid motion is obvious in Figure 3. Appreciation of this parameters accounts for a shortfall in the velocity boundary layer owing to a dragging force contained in the magnetic field number. Hence, these parameters resist and impedes the rate at which fluid flows or circulates. This phenomenon can be noticed in various systems such as nuclear reactors, etc. Figure 4, shows evolution of Grashof number due to convective buoyancy impact. If the heat gradient existing due to the buoyancy force caused by fluid density and limiting force owing to fluid viscidness is enhanced, then the fluid movement is rises.

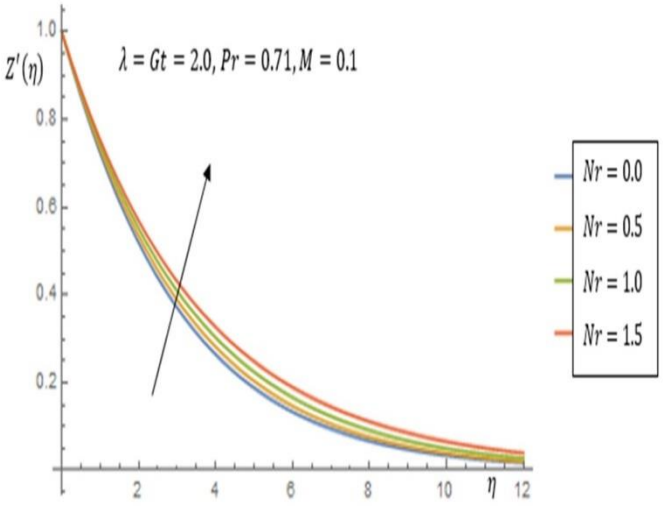

Figure 2. Effect of Radiation Factor, Nr on Velocity

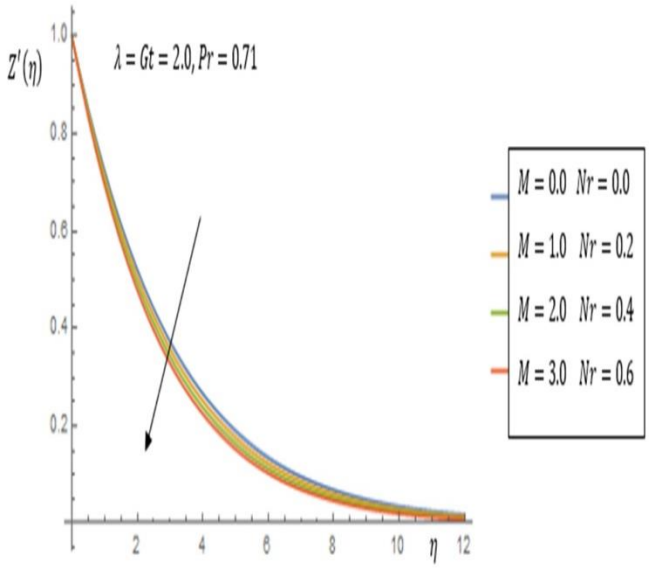

Figure 3. Effect of Magnetic, M and Radiation, Nr parameters on Velocity

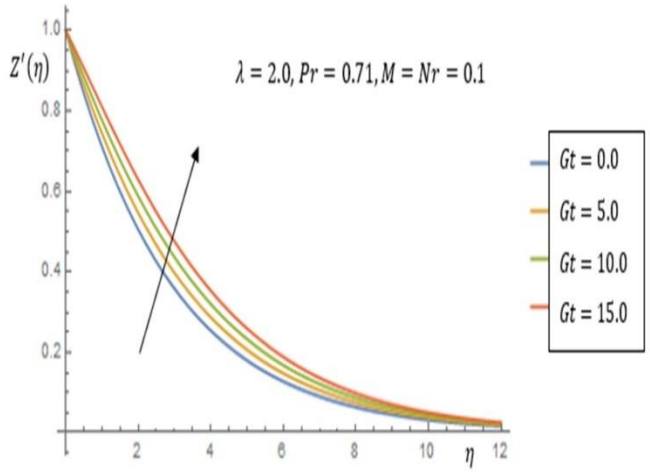

Figure 4. Effect of Heat Grashof parameter, Gt on Velocity

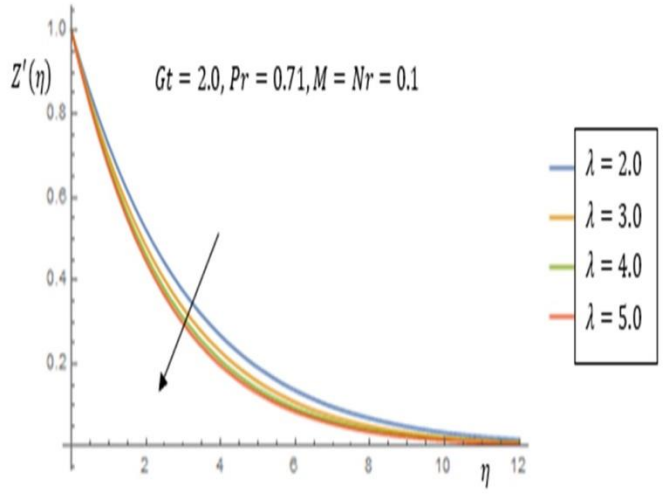

Figure 5. Effect of Casson (Non-Newtonian) parameter, λ on Velocity

The effect of non-Newtonian parameter, λ on the flow distribution is well depicted in Figure 5. Meanwhile, enhancing this parameter suppresses the momentum boundary layer and thereby creating a decline in velocity. In Figure 6, the combined impact of the appreciating values of both λ and M, led to a decline in the thickness of the momentum boundary surface and leads to a diminishing rate of fluid flow.

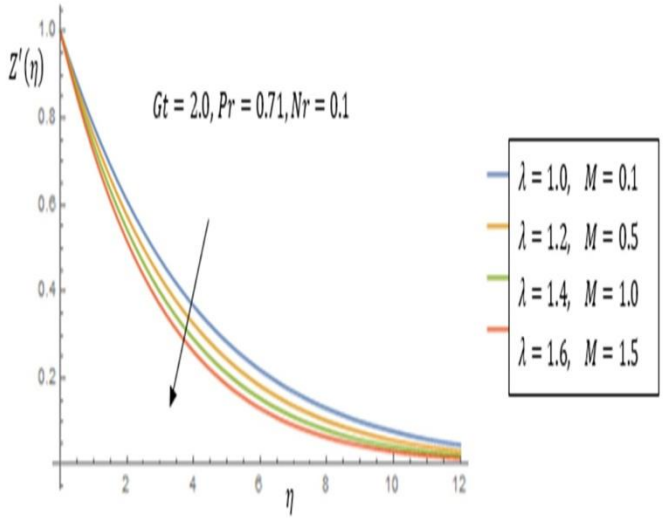

Figure 6. Effect of Casson (Non-Newtonian), λ and Magnetic, M parameters on velocity

The impress of the various vital fluid constraints on temperature is outlined in figures 7 to 10. In Figure 7, the outcome of improving M on the profile is showcased. Unlike, in the case of velocity, the temperature rises as M increases because the heat energy counters the Lorentz force which arises from the magnetic field. Figure 8, denotes the temperature profile due to radiative number, Nr effect. Increasing such a parameter leads to the introduction of extra heat energy into the nanofluid thereby enhancing the fluid's temperature. The outcome of varying the non-Newtonian number, λ on temperature distribution is revealed in Figure 9. Progressive increment in the values of this parameter enhances the boundary layer thermally and the temperature.

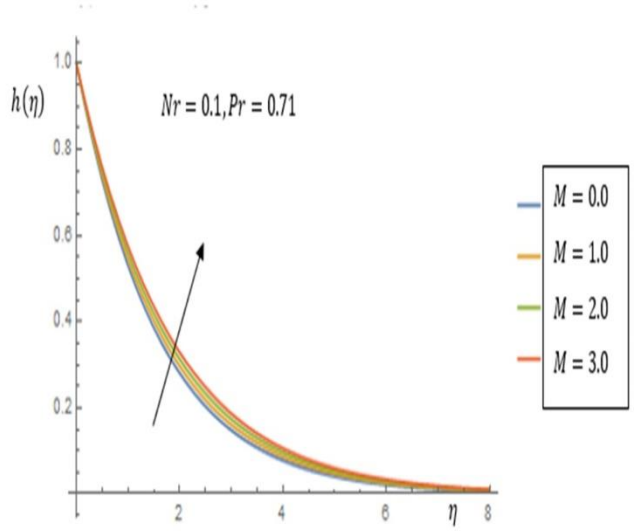

Figure 7. Effect of Magnetic, M parameter on Temperature

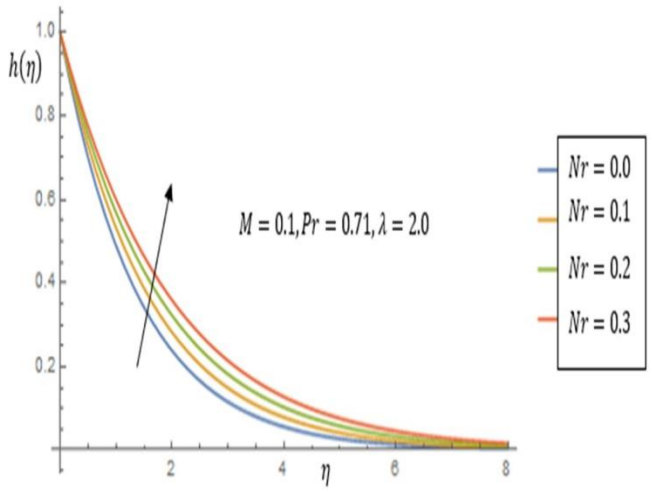

Figure 8. Effect of Radiation factor, Nr on Temperature

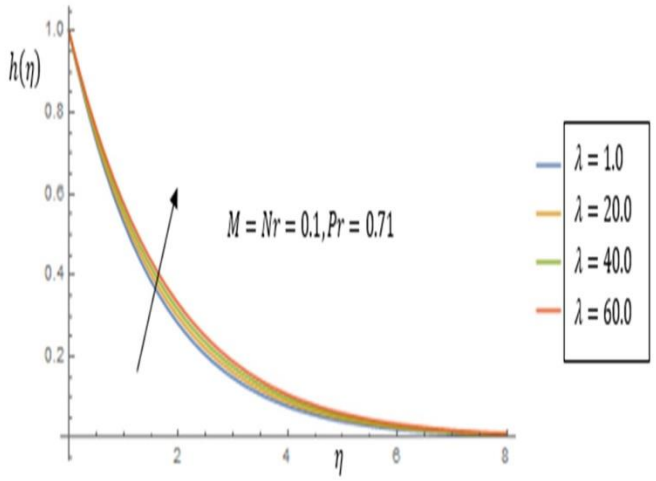

Figure 9. Effect of Non-Newtonian number, λ on Temperature

The impact of Prandtl number on the temperature is shown in figure 10. The relation between Pr of gases ($Pr = 0.71$), air ($Pr = 0.71$) and water ($Pr = 7.0$) at room temperature is made visible in the profile. However, when this number increases to 0.71 (gases) the wall due to heat becomes thicker while temperature circulation decreases. As this value rises from 1.0 to 7.0, for several conducting fluids, the boundary layer becomes thinner just as the temperature flow field continues to decrease. Thus, the lower values of Pr ($Pr < 1$) denotes high thermal diffusivity but for higher values i.e., $Pr \gg 1$, the momentum dispersion controls the pattern of flow.

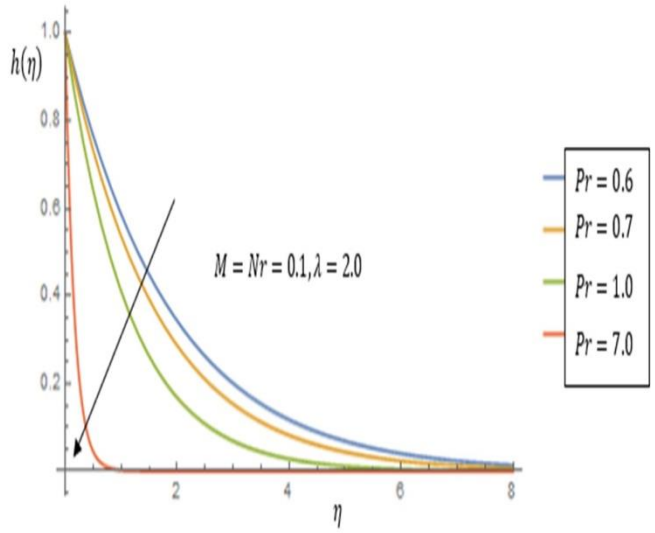

Figure 10. Effect of Prandtl number, Pr on Temperature

The effect of other physical terms against nanoparticle concentration is signified in Figures 11 to 13. Increasing the values of radiation number, Nr leads to an enhancement of the nanoparticle diffusion rate which is caused as a result of an increase in heat energy and presence of surface area in addition to random motion of the nanoparticles. This occurrence is illustrated in Figure 11. The impact of Schmidt number on nanoparticle concentration distribution is visualised in Figure 12. This parameter represents proportionality of momentum diffusion to mass diffusion and it's useful in categorizing fluid distribution arising from concurrent thrust and mass dispersal processes in convective heat transport. Hence, enhancement in its values results to a decaying distribution of the nanoparticle concentration. Meanwhile, the implication of the rising values of the Soret number, Sr is beamed in Figure 13 and it indicates an increment in the nanoparticle concentration as its value improves.

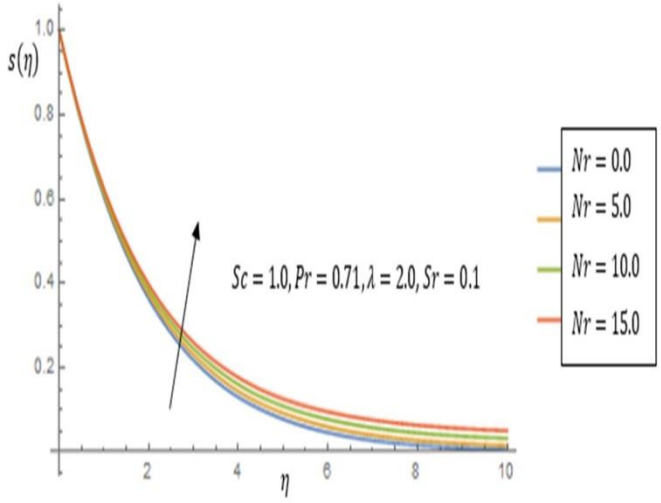

Figure 11. Effect of Radiation factor, Nr on Nanoparticle Concentration

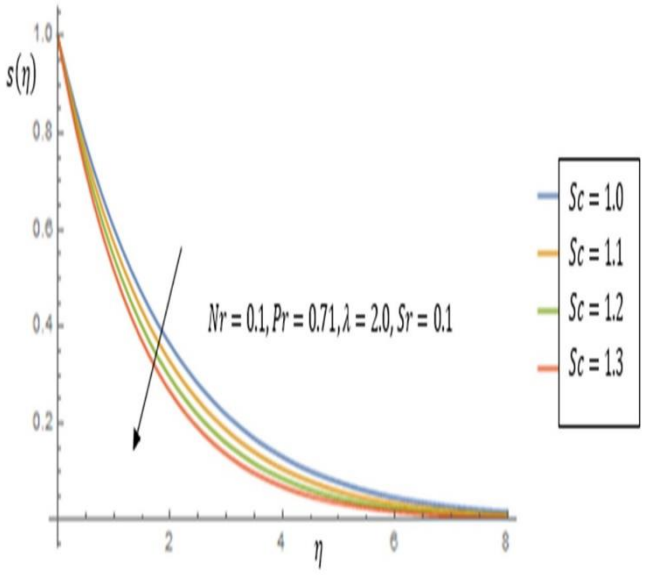

Figure 12. Effect of Schmidt number, Sc on Nanoparticle Concentration

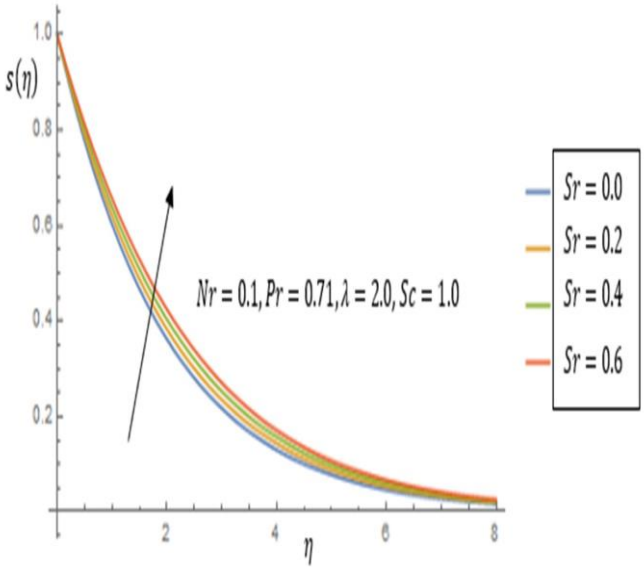

Figure 13. Effect of Soret number, Sr on Nanoparticle Concentration

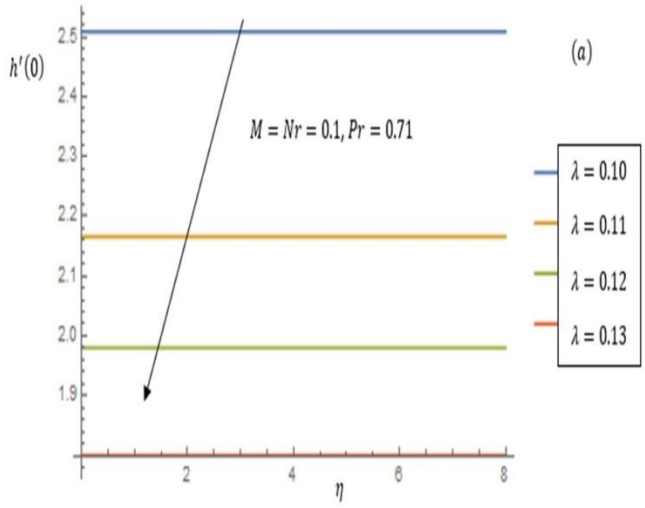

Figure 14 (a). Effect of Non-Newtonian (Casson) number on the Wall temperature gradient, $h'(\eta)$

The significance of the non-Newtonian parameter on the Nusselt and Sherwood numbers are featured in Figures 14 (a) and (b) as well as Tables (a) and (b) respectively. However, as the non-Newtonian parameter intensify, both the wall temperature (Nusselt number) and mass gradients (Sherwood number) declines. This phenomenon can also be noticed from Tables 1 and 2. From this tables, a decreasing trend of both the Nusselt and Sherwood numbers can be seen due to the influence of the non-Newtonian parameter as they increase. However, the rate of receding in Figure (a) is faster than that of Figure (b) since they nanoparticles tends to diffuse slowly than the temperature.

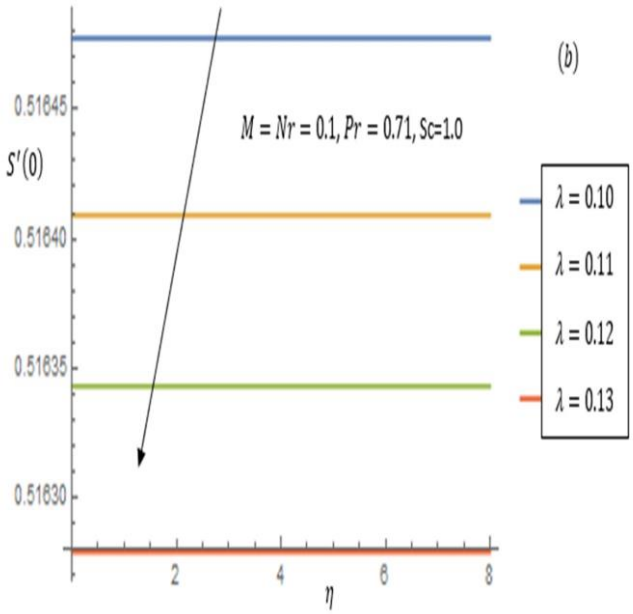

Figure 14 (b). Effect of Non-Newtonian (Casson) number on the Wall mass gradient, $h'(\eta)$

1. **Table 1:** Effect of Non-Newtonian (Casson) number on the Wall with $M = Nr = 0.1$, $Pr = 0.71$

λ	Nu
0.10	3.12488
0.11	2.67862
0.12	2.33912
0.13	2.07470

2. **Table 2:** Effect of Non-Newtonian (Casson) number on the Wall with $M = Nr = 0.1$, $Pr = 0.71$

λ	Sh
0.10	0.51647
0.11	0.51641
0.12	0.51634
0.13	0.51630

Conclusion

In this study, we have deployed the series approximation technique in solving the problem under consideration and this method has proved to be efficient, stable, simple and reliable. From this present study, we have been able to reveal that:

(a) increase in the Soret and radiation factors led to an upsurge in the specie (nanoparticle) mass.
(b) the Prandtl parameter is vital in controlling the rate of cooling especially in a conducting fluid. Thus, at $Pr < 1$, heat diffuses more than in the case of $Pr > 1$.
(c) in order to reduce the rate of fluid movement in a given mechanical machine, engines etc., the non-Newtonian

number, λ becomes very useful just as it rises in value while the momentum boundary layer becomes thinner.

(d) There is an enhancement of the boundary layer due to thermal energy which leads to an intensification of fluid temperature.

(e) as the non-Newtonian number surges, both the thickness of the thermal and mass wall layers degenerate.

However, this study is limited to a steady case of fluid transmission. Thus, an extension of it to the unsteady case can form a future case study. The application of this research ranges from solar power, nuclear fluidization, cable annealing, spinning of glasses, targeting of drugs to cancer-tumor affected areas of the body (done with an improved advanced technology) for treatment, oil exploration, cooling of automobiles radiators cum engines etc.

Conflict of Interest

The authors have confirmed that there is no conflict of interest mentioned.

Acknowledgement

We sincerely thank the reviewers for their thorough criticism and suggestions.

References

[1] Dash, R. K., Mchta, K. N., Jayaraman, G., (1996), Casson fluid flow in a pipe filled with a homogeneous porous medium., Int. J. Eng. Sci., **34(10**), 1145-1156.

[2] Choi, S. U. S., Eastman, J. A., (1995), Enhancing thermal Conductivity of fluids with nanoparticles, Agonne IL, National Lab. (United States), 196525 ANL/MSD/CP-84938: CONF-951135-29, NO: DE96004174: TRN: 96: 001707: Conference: International mechanical engineering congress and exhibition, San Francisco, CA.

[3] Uka, U. A., Emeka, A., Chinedu, N., (2022). Chemical reaction and thermal radiation effects on exponentially stretching sheet., Ther Maths. and Appl., **12(2),** 1-19. https://doi.org/10.47260/tma/1221.

[4] El-Aziz, M. A., (2009), Viscous dissipation effect on mixed convection flow of a micropolar fluid over an exponentially stretching sheet., Can. J. Phys., **87**, 359-368.

[5] Mukhopadhyay, S., Gorla, R. S. R., (2012), Effects of partial slip on boundary layer flow past a permeable exponential stretching sheet in the presence of thermal radiation., Heat Mass Transfer., **48(10)**, 1773-1781. https://dx.doi.org/10.1007/s00231-012.1024-8.

[6] Serdar, B., Salih, D. M., (2006), Three-Dimensional stagnation point flow of a second-grade fluid towards a moving plate., Int. J. Sc., **44**, 49-58.

[7] Amos, E., Uka, U. A., (2022), Hydromagnetic nanofluid flow over an exponentially stretching sheet in the presence of radiation and non-uniform heat generation and absorption., IOSR Journal of Mathematics., **18(1)**, 31-43. https://doi.org/10.9790/5728-1801023143.

[8] Hassan, M., Marin, M., Alsharif, A., Ellahi, R., (2018), Convective heat transfer flow of nanofluid in a porous medium past curly surface., Phys. Letters A., **382(38)**, 2749-2753.

[9] Kataria, H. R., Patel, H. R., (2018), Heat and mass transfer in MHD Casson fluid flow over an oscillating upright plate immersed in porous medium with ramped wall temperature., Prop. Pow. Res., **7(9)**, 257-267.

[10] Abd El-Aziz, M., Afify, A. A., (2019), Casson fluid flow over a stretching sheet with entropy generation analysis and hall influence., Entropy., **21(6)**, 592. https://dx.doi.org/10.3390/e21060592.

[11] Khan, K. A., Raza, N., Inc, M., (2021), Insights of numerical simulations of MHD squeezing nanofluid flow across a channel with porous walls., Pro. Power Research., **1**, 146-154.

[12] Beg, O. A., Tripathi, D., (2012), Mathematical simulation of peristaltic pumping with dual-diffusivity convection in nanofluids: a bio-nano engineering model., proceedings of the Institution of mechanical engineers-part N., Journal of Nano-engineering and Nano-systems., **225(3)**, 99-114.

[13] Tripathi, D., Beg, O. A., (2014), A study on peristaltic flow of nanofluids: application in drug delivery systems., Int. J. Heat and Mass Trans., **70**, 61-70.

[14] El-Dabe, N. T., Abou-Zeid, M. Y., El-Kalaawy, O. H., Moawad, S. M., Ahmad, O. S., (2019), Electromagnetic steady motion of Casson fluid with heat and mass transfer through a porous medium over a shrinking surface., Thermal Science., **25(1)**, 257-265.

[15] Pal, D., Mondal, H., (2010), Hydro-magnetic non-Darcy flow and heat transfer over a stretching sheet in the presence of thermal radiation and Ohmic dissipation., Communications in Non-linear Science and Numerical Simulation., **15(5)**, 1197-1209.

[16] Pramanik, S., (2014), Casson fluid flow and heat transport over an exponentially porous stretching surface with radiation., Ain Shams Engineering Journal., **5(1)**, 205-212.

[17] Durgaprasad, P., Varma, S. V. K., Hoque, M. M., Raju, C. S. K., (2019), Combined effects of Brownian motion and thermophoresis numbers on 2D Casson fluid flow over a spongy layer insulating sheet in a mixture of graphite nanoparticles., Neural Comput. App., **31(10)**, 6275-6286.

[18] Anantha, K. K., Saneep, N., Sugunama, Y., Animasaun, I. L., (2020), Effect of asymmetrical thermal generation/absorption on the radiation thin film flow of MHD ferro-fluid mixture., J. Therm. Anal. Calorim., **139(3)**, 2145-2153. https://doi.org/10.1007/s10973-019-08628-4.

[19] Sulochana, C., Apana, S. R., (2019), Unsteady MHD radiation flow past a boundless permeable sheet in the presence of Hall current and chemical reaction., Adv. Sci. Eng. Med., **11(6)**, 537-548. https://doi.org/10.1166/asem.2383.

[20] Das, M., Mahanta, G., Shaw, S., Parida, S. B., (2019), Unsteady MHD chemically reactive double-diffusive Casson fluid past a flat plate in a porous with heat and mass transfer., Heat Trans., **48(5),** 1761-1777. http://doi.org/10.1002/htj.21456.

[21] Raju, C. S. K., Sandeep, N., Sugunamma, V., Babu, M. J., Reddy, J. V. R., (2015), Heat and mass transfer in MHD Casson fluid over an exponentially permeable stretching surface., Eng. Sci. and Tech., an international Journal., http://dx.doi:10.1016/j.jestech.2015.05.010.

[22] Kashif, A. K., Faizan, J., Javaid, A., IIyas, K., Nauman, A., Mulugeta, A., Muhammad, R., (2022), Analytical simulation of heat and mass transportation in Casson fluid flow over a stretching surface., Mathematical Problems in Engineering., Article ID: 5576194, 11 pages. http://doi/10.1155/2022/5576194.

[23] Nadeem, S., Haq, R. I., Akbar, N. S., Khan, Z. H., (2013), MHD three dimensional Casson fluid flow past a porous linearly stretching sheet., Alex. Eng. J., **52**, 57-582.

[24] Mukhopadhyay, S., Bhattacharyya, K., Hayat, T., (2013), Exact solutions for the flow of Casson fluid over stretching surface with transpiration and heat transfer effects., Chin. Phys. B., **22(11)**, 114701. DOI: 10.1088/1674-1056/22/11/114701.

[25] Bestman, A. R., (1990), The boundary- layer flow past a semi-infinite heated plate for two-component plasma., Astrophysics and space science., **173**, 93-100.

Abbreviations and Acronyms

N_b	Brownian motion parameter
K_r	chemical reaction rate parameter
Q_s	heat source/sink parameter
C_p	heat capacity at constant pressure ($J\ kg^{-1}K^{-1}$)
M	magnetic field number
Q_s	heat source/sink parameter
C	local nanoparticles mass concentration ($kg\ m^{-3}$)
B_0^2	magnetic field strength
C_w	nanoparticle concentration at the plate ($kg\ m^{-3}$)
C_∞	nanoparticle mass concentration far away from the plate ($kg\ m^{-3}$)
U	non-dimensional free stream velocity (ms^{-1})
D_B	molecular mass coefficient (m^2s^{-1})
Pr	Prandtl number
S	radiation parameter
Sc	Schmidt number
J_t	thermal Grashof parameter
N_t	thermophoresis factor
MHD	Magnetohydrodynamics
$PDEs$	Partial Differential Equations
$ODEs$	Ordinary Differential Equations
DE	Differential Equation
h	Non-dimensional fluid temperature
S	Dimensionless fluid concentration
Z'	Non-dimensional velocity
HAM	Homotopy analysis method.
3D	Three dimensional
DEs	Differential equations